Supporting Information for:

Tetrahedral Sn-Silsesquioxane: synthesis, characterization and catalysis

Contents **Page**

Experimental

(POSS-^{i}Bu$_7$-Sn-Me)$_2$·Et$_2$NH·H$_2$O dimer A flask was loaded with POSS-^{i}Bu$_7$-(OH)$_3$ (0.98 g, 1.2 mmol), diethylamine (0.50 mL, 4.8 mmol) and diethyl ether (20 mL). A solution of methyltin trichloride (0.30 g, 1.2 mmol) in diethyl ether (5.0 mL) was added to the flask dropwise upon vigorous stirring. Lots of white precipitate (Et$_2$NH$_2$Cl) formed. The mixture was stirred for 2 hours, and filtered to give a colorless filtrate. The volatiles were removed under vacuum to yield a white crystalline material. Yield: 0.73 g (65%). 0.20 g of this product was recrystallized from CH$_2$Cl$_2$/CH$_3$CN (4 mL/12 mL) at 4 ^{o}C, and 0.12 g single crystalline materials were obtained (recrystallization yield:

60%). ^{1}H NMR ($CDCl_3$, 400 MHz): δ 8.19 (br s, 2H, $\mathrm{Et_2N}H_2^+$); 4.75 (br s, 1H, O*H*); 3.25 (br, 4H, $\mathrm{CH_3C}H_2\mathrm{N}$); 1.85 (m, 14H, $\mathrm{-CH_2C}H\mathrm{(CH_3)_2}$); 1.33 (t, 6H, *J* = 6.9, $\mathrm{C}H_3\mathrm{CH_2N}$); 0.97 – 0.92 (overlapped d, 84H, *J* = 6.2, $\mathrm{-CH_2CH(C}H_3\mathrm{)_2}$); 0.64 (s, 6H, Sn-$\mathrm{C}H_3$); 0.63 – 0.32 (overlapped d, 28H, *J* = 6.9, $\mathrm{-C}H_2\mathrm{CH(CH_3)_2}$). ^{13}C NMR ($CDCl_3$, 100 MHz): δ 38.27; 26.70; 26.26; 26.21; 26.18; 26.07; 25.89; 25.36; 25.15; 24.68; 24.65; 24.38; 24.18; 24.08; 23.23; 10.42; 8.04. ^{29}Si NMR ($CDCl_3$, 79 MHz): δ -65.17; -66.04; -66.19; -66.91; -69.96. ^{119}Sn NMR ($CDCl_3$, 149 MHz): δ -533.61. Anal. Calcd. for $C_{62}H_{145}NO_{25}Si_{14}Sn_2$: C, 38.48; H, 7.55; N, 0.72. Found: C, 38.06; H, 7.27; N, 0.68.

POSS-(*c*-hexyl)$_7$-vinyl-(OH)$_2$, compound 2. To a solution of POSS-(*c*-hexyl)$_7$-(OH)$_3$ (1.94 g, 2.00 mmol) in THF (20 mL) triethylamine (0.42 mL, 3.0 mmol) was added and the mixture was cooled to -15 °C with an aid of ice-salt bath. Chlorovinyldimethylsilane (0.33 mL, 2.4 mmol) was added dropwise at -15 °C and the resulting slurry was allowed to warm up to room temperature. After stirring for 30 min the mixture was filtered through a syringe filter and evaporated in vacuo. Hexanes (25 mL) was added and the cloudy solution was filtered through a syringe filter, evaporated and dried in vacuo to afford the product as a white powder (1.762 g, 83%). ^{1}H NMR ($CDCl_3$, 400 MHz) δ 6.20 (dd, *J* = 20.3, 14.9 Hz, 1H), 5.99 (dd, *J* = 14.9, 3.9 Hz, 1H), 5.81 (dd, *J* = 20.3, 4.0 Hz, 1H), 1.82 – 1.65 (m, 35H), 1.33 – 1.15 (m, 35H), 0.75 (m, 7H), 0.22 (s, 6H). ^{13}C NMR (101 MHz, $CDCl_3$) δ 139.35, 132.72, 27.62, 27.59, 27.53, 27.49, 26.88, 26.85, 26.84, 26.79, 26.65, 26.59, 26.54, 24.53, 23.87, 23.47, 23.18, 23.06, 0.03. ^{29}Si NMR (79 MHz, $CDCl_3$) δ -1.23, -58.85 (2), -67.69, -67.88, -68.41, -69.75 (2). HRMS (ESI) *m/z* calcd for $C_{46}H_{89}O_{12}Si_8$ $(M+H)^+$ 1057.4503, found 1057.4520.

(*c*-hexyl)-POSS-Sn-POSS, compound 3. To a solution of compound **2** (208 mg, 0.197 mmol) in dry toluene (10 mL) was added Sn(O*i*Pr)$_4$·*i*PrOH (43.7 mg, 0.123 mmol) in dry toluene (1.5 mL) dropwise over the period of 30 min. The mixture was heated up to 100 °C and stirred in the flow of nitrogen to remove the volatiles. Drying at 100 °C under high vacuum afforded the product (219 mg, 99.6%) as a light yellow powder. ^{1}H NMR (500 MHz, $CDCl_3$) δ 6.14 (dd, *J* = 20.4, 14.8 Hz, 1H), 5.91 (dd, *J* = 14.8, 4.0 Hz, 1H), 5.72 (dd, *J* = 20.4, 4.0 Hz, 1H), 1.86 – 1.64 (m, 35H), 1.32 – 1.12 (m, 35H), 0.81 – 0.59 (m, 7H), 0.20 (s, 3H), 0.19 (s, 3H). ^{13}C NMR (126 MHz, $CDCl_3$) δ 139.40, 131.54, 27.82, 27.77, 27.73, 27.69, 27.63, 27.60, 27.55, 27.52, 27.45, 27.40, 27.06, 26.97, 26.93, 26.90, 26.85, 26.78, 26.67, 26.60 (CH_2's of *c*-hexyl), 24.82, 24.76, 24.64 (2), 24.18, 23.14, 23.10 (CH's of *c*-hexyl), 0.44, 0.35 (CH_3's). ^{29}Si NMR (79 MHz, $CDCl_3$) δ -1.87, -62.50, -63.46, -67.28, -67.71, -67.94, -70.10, -70.54. ^{29}Si NMR (79 MHz, toluene-d_8) δ -1.36, -61.85, -62.81, -66.57, -67.00, -67.44, -69.43, -69.91. ^{119}Sn NMR (149 MHz, toluene-d_8) δ -438.8. HRMS (ESI) *m/z* calcd for $C_{92}H_{173}O_{24}Si_{16}$ $(M+H)^+$ 2230.7661, found 2230.7664.

Interactions with external ligands. Solutions of **3** in $CDCl_3$ were prepared in the nitrogen atmosphere of the glovebox and placed into J Young tubes. Concentrations of **3** were determined by ^{1}H NMR using hexamethylbenzene as an internal standard. The solutions were titrated with ligands using microsyringe in the nitrogen glovebox and the NMR data were collected.

Styrene oxide ring-opening reaction. Under the nitrogen atmosphere of the glovebox, to a mixture of styrene oxide (0.10 mL, 0.87 mmol) and benzyl alcohol (0.10 mL, 0.97 mmol) was added **3** (4.5 μmol, 0.5 mol %) as a solution in toluene (0.20 mL). The reaction vial was sealed and heated at 80 °C for 16h. ^{1}H and ^{13}C NMR analysis revealed complete consumption of styrene oxide and that the major components of the reaction mixture (>5%) are benzyl alcohol (60% to starting epoxide), 2-(benzyloxy)-2-phenyl-ethanol (50%)[1] and phenethyl alcohol (10%). Less than 0.5% of the product was observed in a control experiment performed without the catalyst at 100 °C for 16h.

Hydride transfer reaction. Under the nitrogen atmosphere of the glovebox, to a mixture of *p*-nitrobenzaldehyde (45.2 mg, 0.299 mmol) and benzyl alcohol (0.00 mL, 0.97 mmol) was added **3** (4.5 μmol) as a solution in toluene (0.20 mL). The reaction vial was sealed and heated at 100 °C for 1h. ^{1}H NMR analysis indicated 95% conversion of *p*-nitrobenzaldehyde to *p*-nitrobenzyl alcohol with a concurrent oxidation of benzyl alcohol to benzaldehyde. No reaction was observed in a control experiment performed without the catalyst at 100 °C for 16h.

X-ray absorption spectroscopy. X-ray absorption measurements were acquired at the Sn K-edge (29.200 keV) on the bending magnet beam line of the Materials Research Collaborative Access Team (MRCAT) at the Advanced Photon Source, Argonne National Laboratory. The data was collected in transmission step-scan mode. Photon energies were selected using a water-cooled, double-crystal Si (111) monochromator, which was detuned by approximately 50 % to reduce harmonic reflections. The ionization chambers were optimized for the maximum current with linear response (~10^{10} photons detected/sec) with 10 % absorption in the incident ion chamber and 70 % absorption in the transmission X-ray detector. A Sn foil spectrum was acquired simultaneously with each sample measurement for energy calibration.

XANES spectra of compound **3** and reference compounds with different oxidation states (SnO_2, $SnCl_2$, $SnCl_4$, $Sn(O^iPr)_4$ were measured. The edge energy and the oxidation states are summarized in Table S2. The coordination numbers and bond distances were determined from the EXAFS data. Solid samples were pressed into a cylindrical sample holder consisting of six wells, forming a self-supporting wafer. Air sensitive samples were prepared in a N_2 glove box. Solid samples were diluted with boron nitride to achieve an absorbance (µx) of approximately 1.0. $SnCl_4$ and the complex **3** dissolved in benzene or toluene were measured as liquids in NMR tubes.

Standard data reduction techniques were employed to fit the data using the WINXAS 3.1 software program. The normalized, energy–calibrated absorption spectra were obtained using standard methods. The edge energy was determined from the maximum of the first peak by taking the first derivative of the XANES spectrum. The EXAFS parameters were obtained by a least square fit in *k*-space of the k^2-weighted isolated first shell Fourier Transform data from Δk = 2.7-10.2 Å^{-1} and ΔR =1.1-1.8 Å. Phase and amplitude fitting functions were determined from SnO_2 to fit compound **3**. SnO_2 is slightly tetragonally distorted (4 Sn-O at 2.058 Å and 2 Sn-O at 2.048 Å) but as the bond lengths differ by only 0.01 Å, we assumed 6 equal bonds (6 Sn-O at 2.05 Å)[2]. Fitted EXAFS parameters are shown in Table S3. The magnitude of the Fourier Transforms for SnO_2, compound **3** are shown in Figure S5a and *k*-space fits of compound **3** fitted with SnO_2 is shown in Figures S5b.

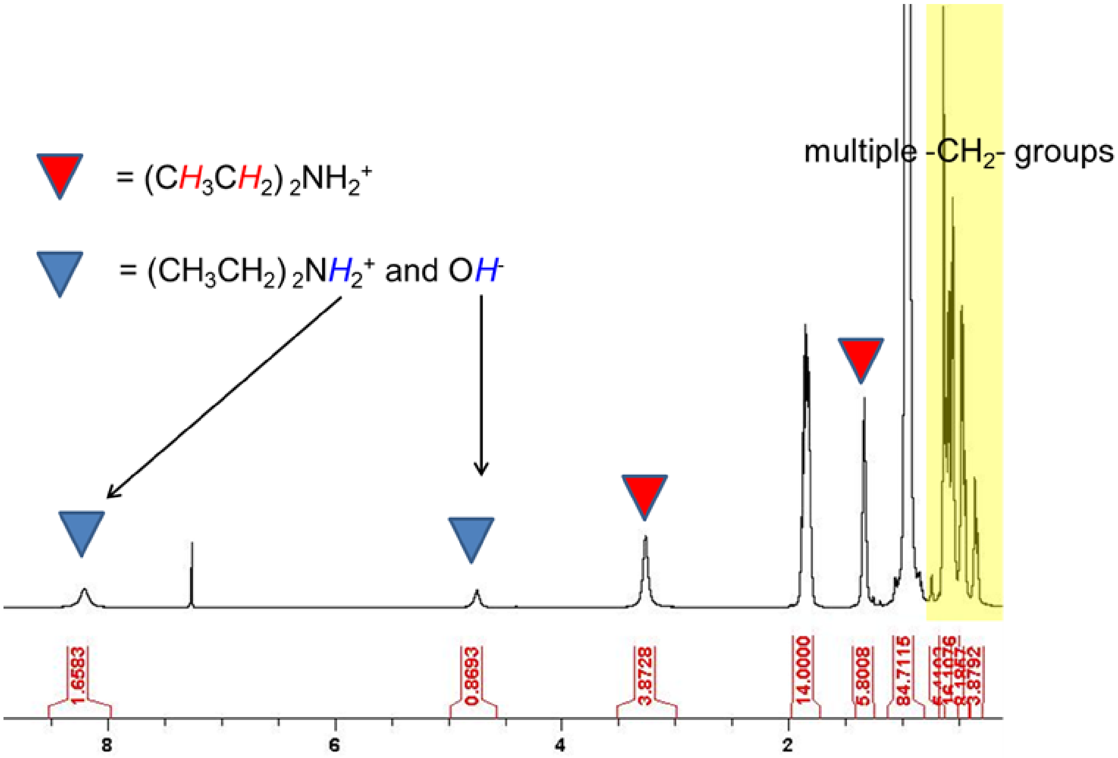

Figure S1a. ^{1}H NMR (POSS-iBu$_7$-Sn-Me)$_2$·Et$_2$NH·H$_2$O dimer in CDCl$_3$.

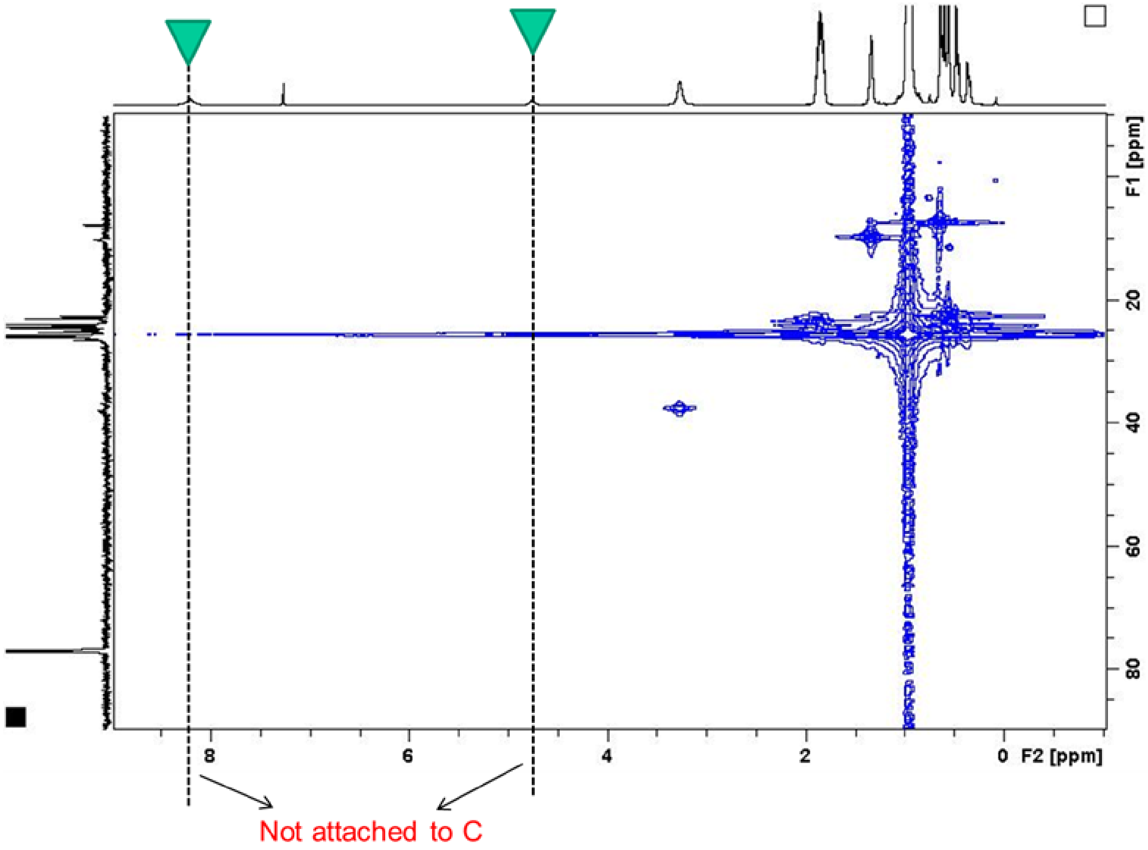

Not attached to C

Figure S1b. ^{1}H-^{13}C HMQC NMR (POSS-iBu$_7$-Sn-Me)$_2$·Et$_2$NH·H$_2$O dimer in CDCl$_3$ confirmed that the two protons at ppm 8.19 and 4.75 were not attached to carbon.

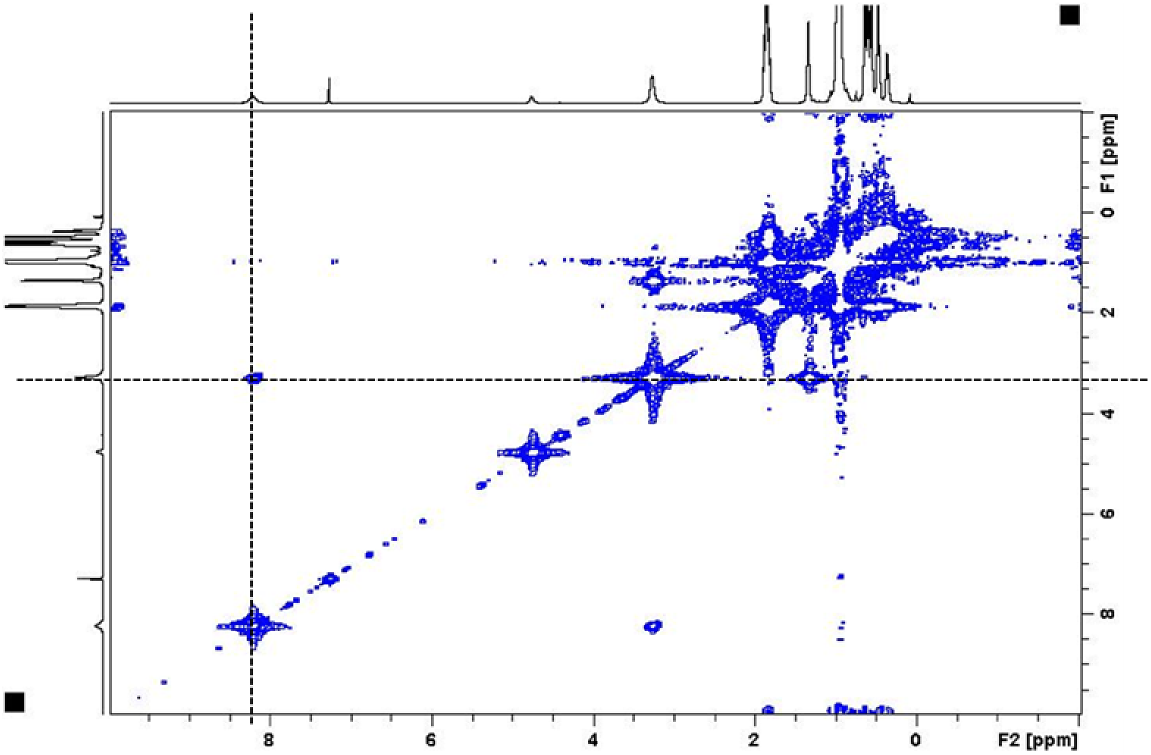

Figure S1c. COSY NMR (POSS-iBu$_7$-Sn-Me)$_2$·Et$_2$NH·H$_2$O dimer in CDCl$_3$ confirmed that the peak at δ 8.19 belong to Et$_2$NH$_2^+$.

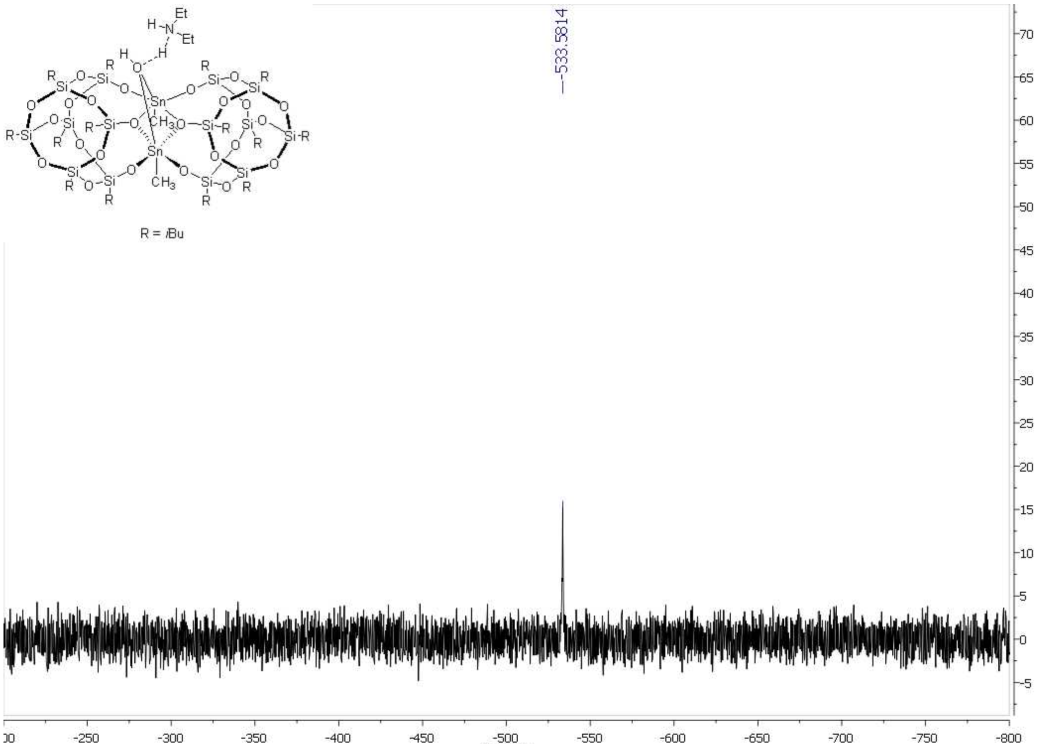

Figure S1d. ^{119}Sn NMR of (POSS-iBu$_7$-Sn-Me)$_2$·Et$_2$NH·H$_2$O dimer.

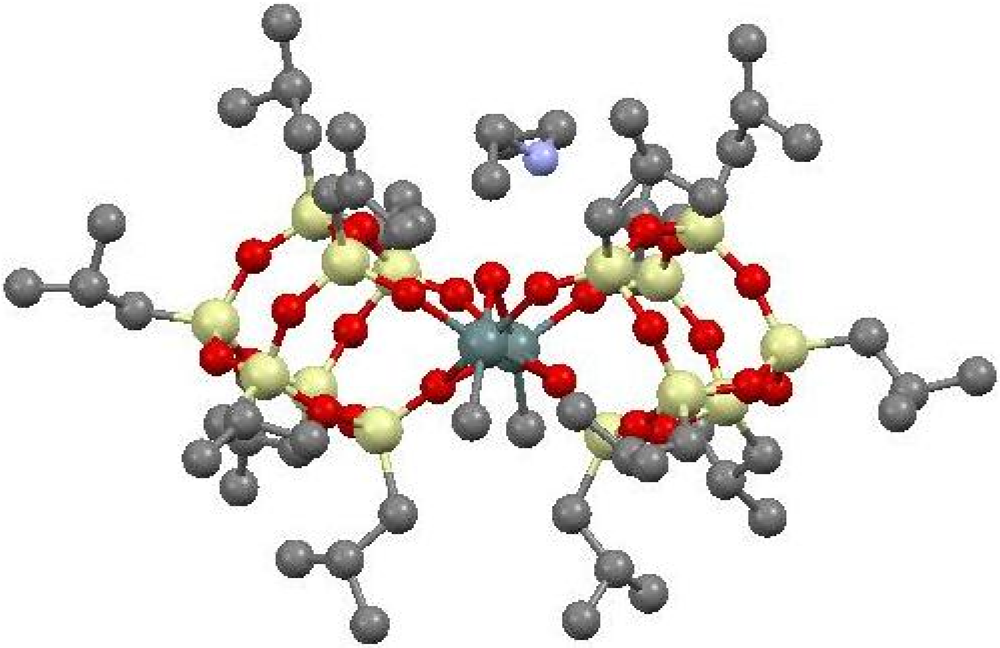

Figure S1e. X-ray crystal structure of (POSS-^{i}Bu$_7$-Sn-Me)$_2$·Et$_2$NH·H$_2$O dimer.

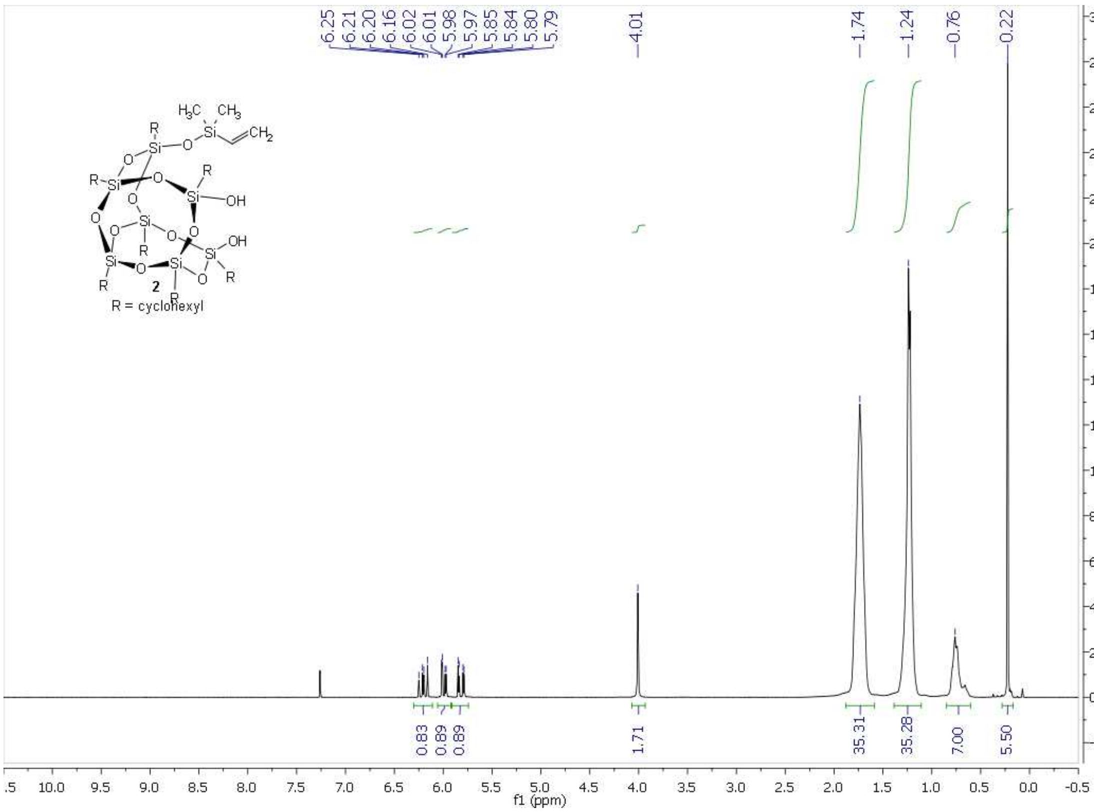

Figure S2a. ^{1}H NMR of compound **2** in CDCl$_3$.

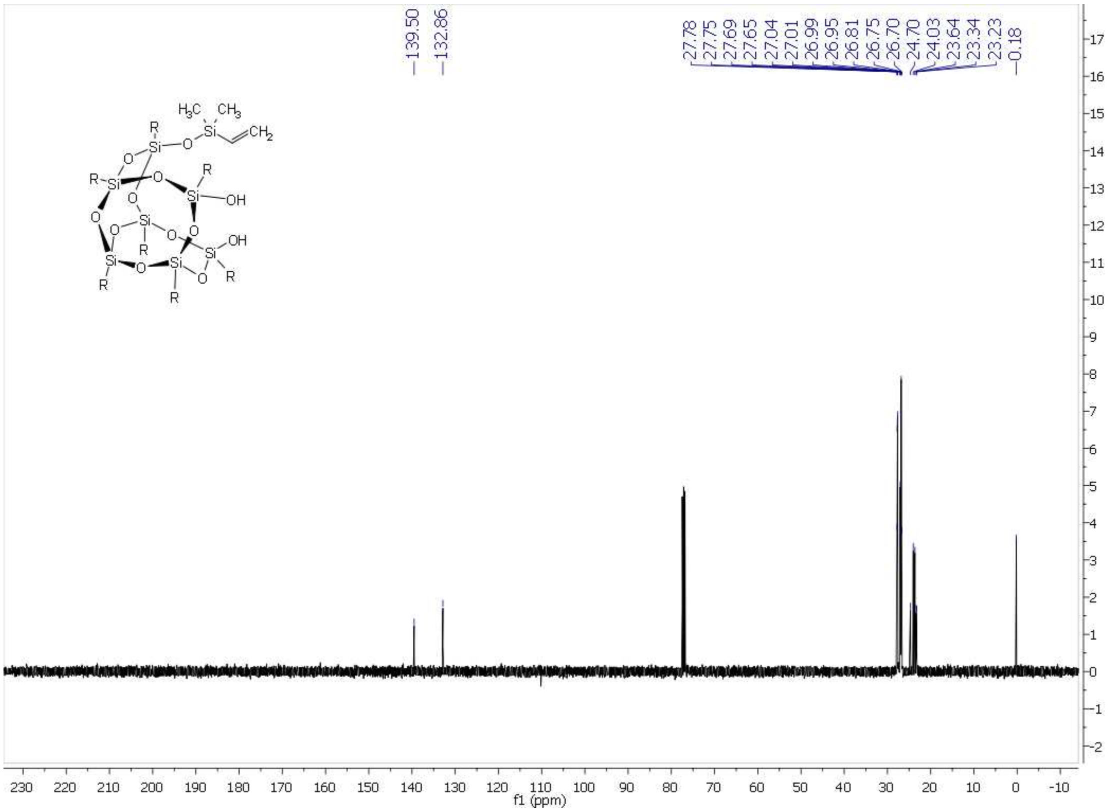

Figure S2b. ^{13}C NMR compound **2** in $CDCl_3$.

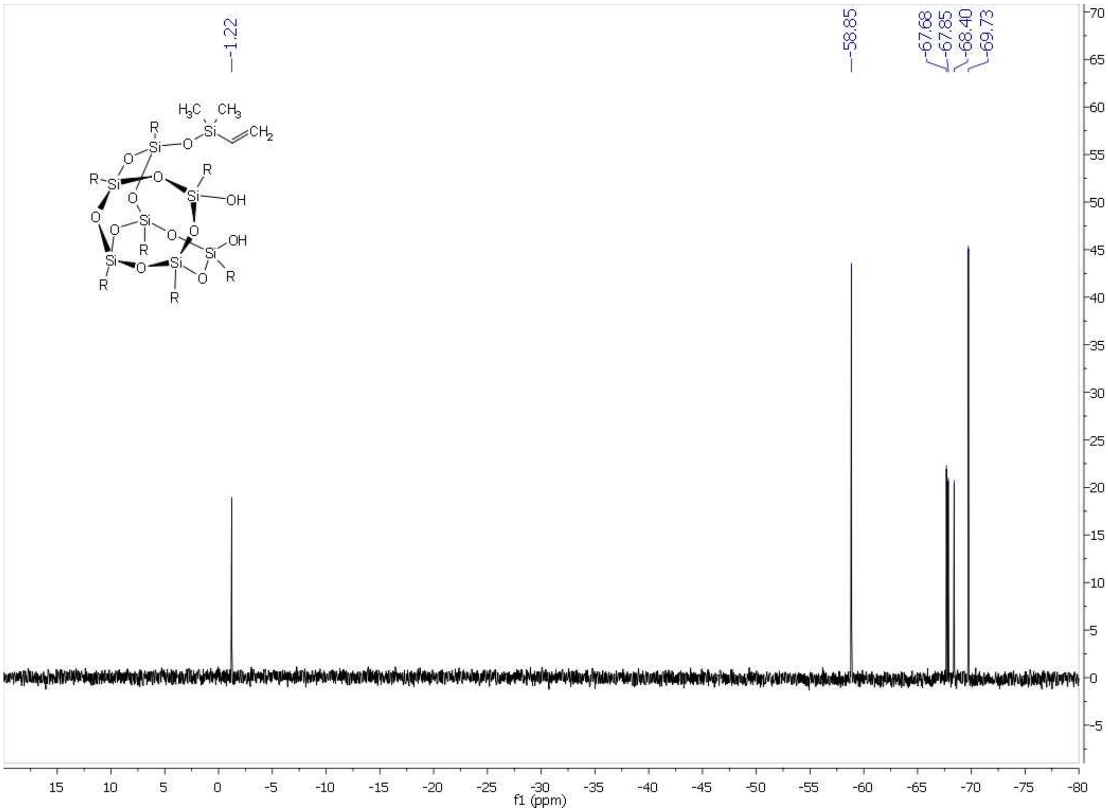

Figure S2c. ^{29}Si NMR compound **2** in $CDCl_3$.

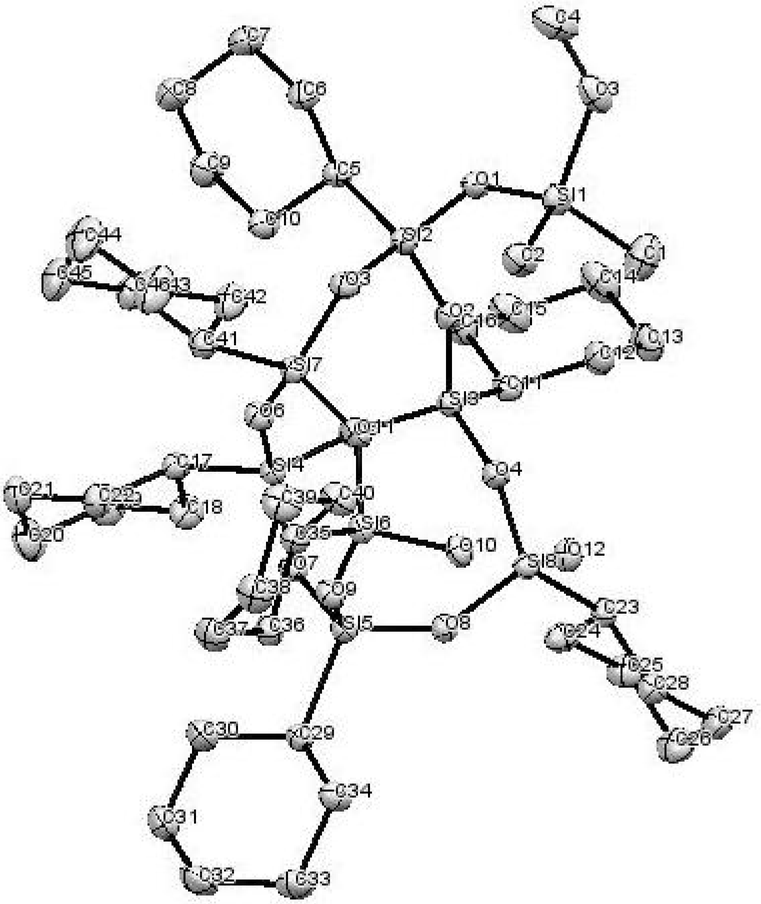

Figure S2d. ORTEP of POSS-*c*-hexyl-vinyl-(OH)$_2$ (2) showing 50% occupancy of the ellipsoid. Protons and minor distorting components atoms not shown for clarity.

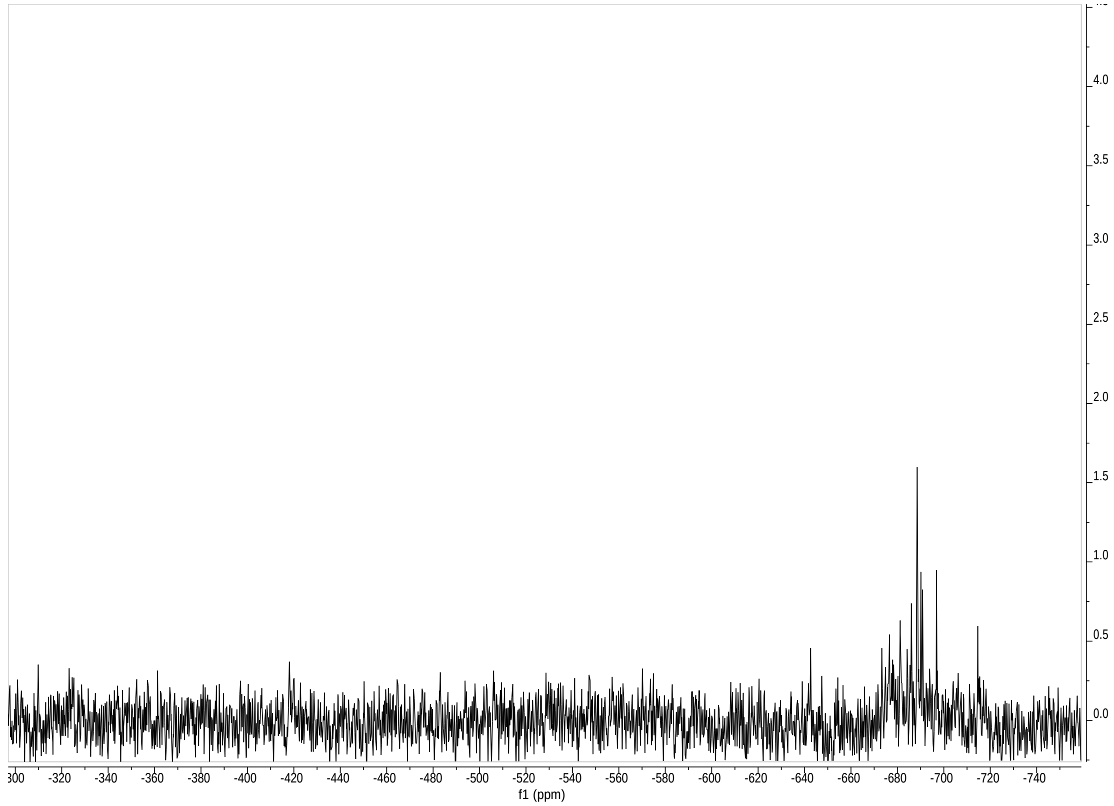

Figure S3a. ^{119}Sn NMR of mixture formed after addition of $Sn(O^iPr)_4 \cdot iPrOH$ to (i-butyl)$_8Si_8O_{11}(OH)_2$.

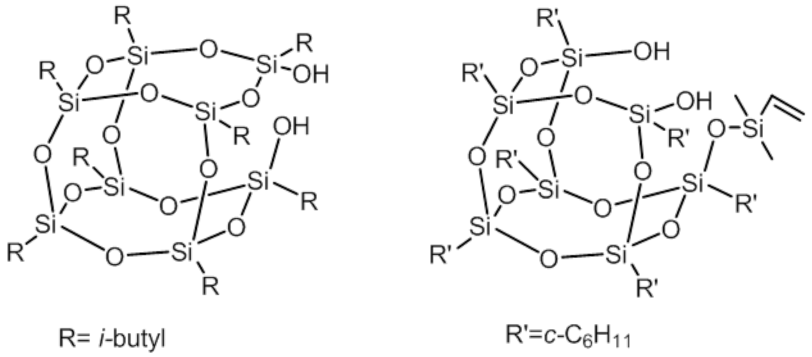

Figure S3b. Structures of (i-butyl)$_8Si_8O_{11}(OH)_2$ and (c-hexyl)$_7Si_7O_7$($OSiC_2H_3Me_2)_2$-$(OH)_2$

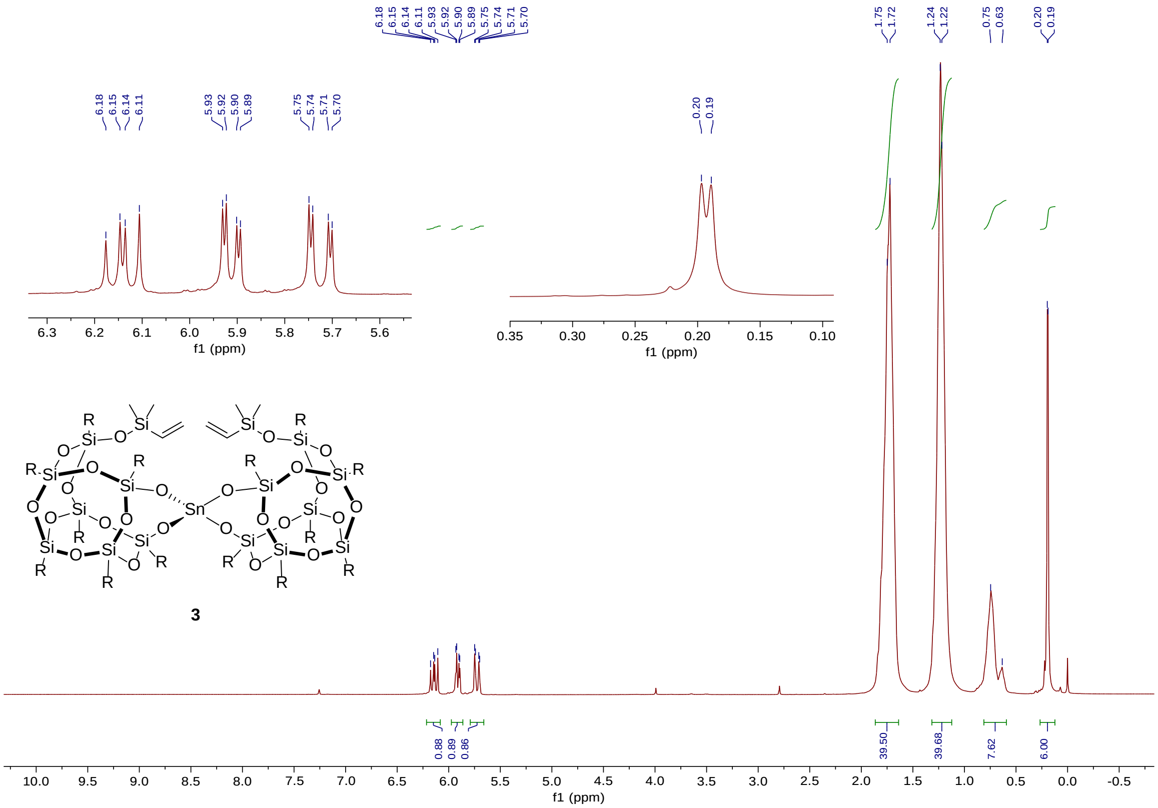

Figure S4a. ^{1}H NMR spectra of **3** in CDCl$_3$. The resonances of the two diastereotopic methyl carbon of $-SiC_2H_3Me_2$ are at δ 0.19 and 0.20 ppm.

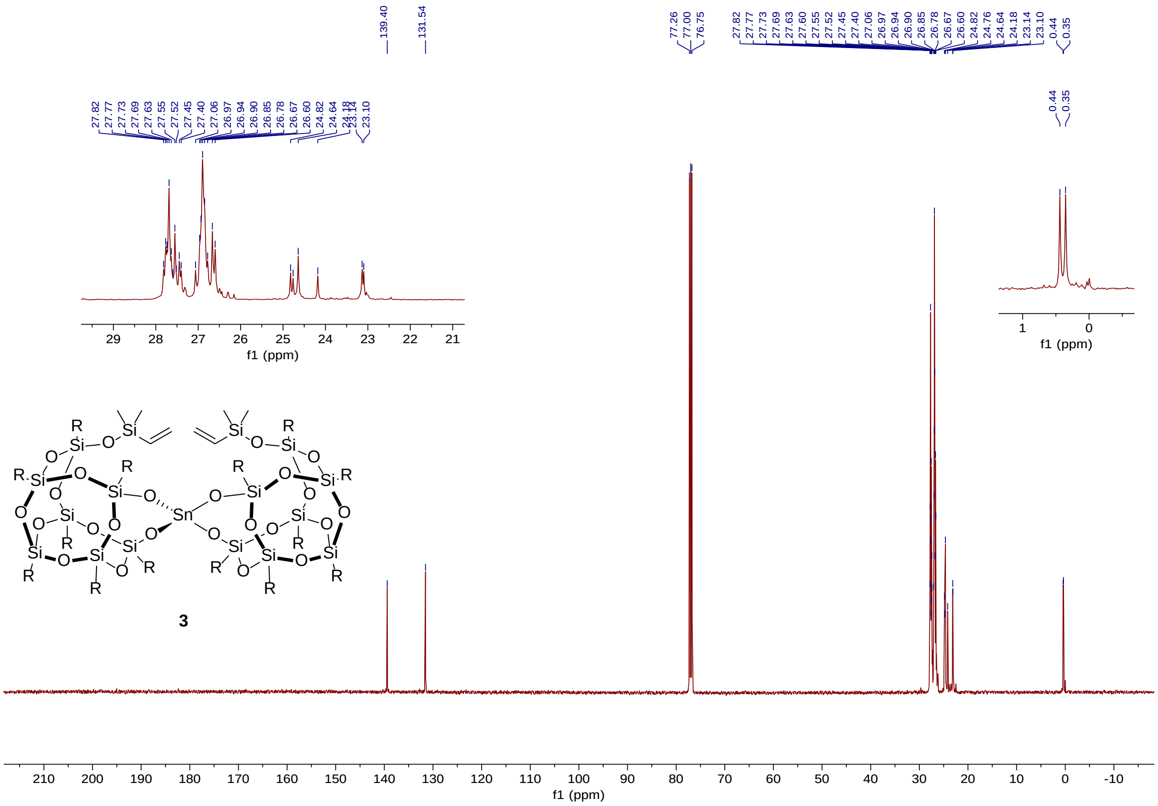

Figure S4b. ^{13}C NMR spectra of **3** in $CDCl_3$. The resonances of the two diastereotopic methyl carbon of $-SiC_2H_3Me_2$ are at δ 0.35 and 0.44 ppm.

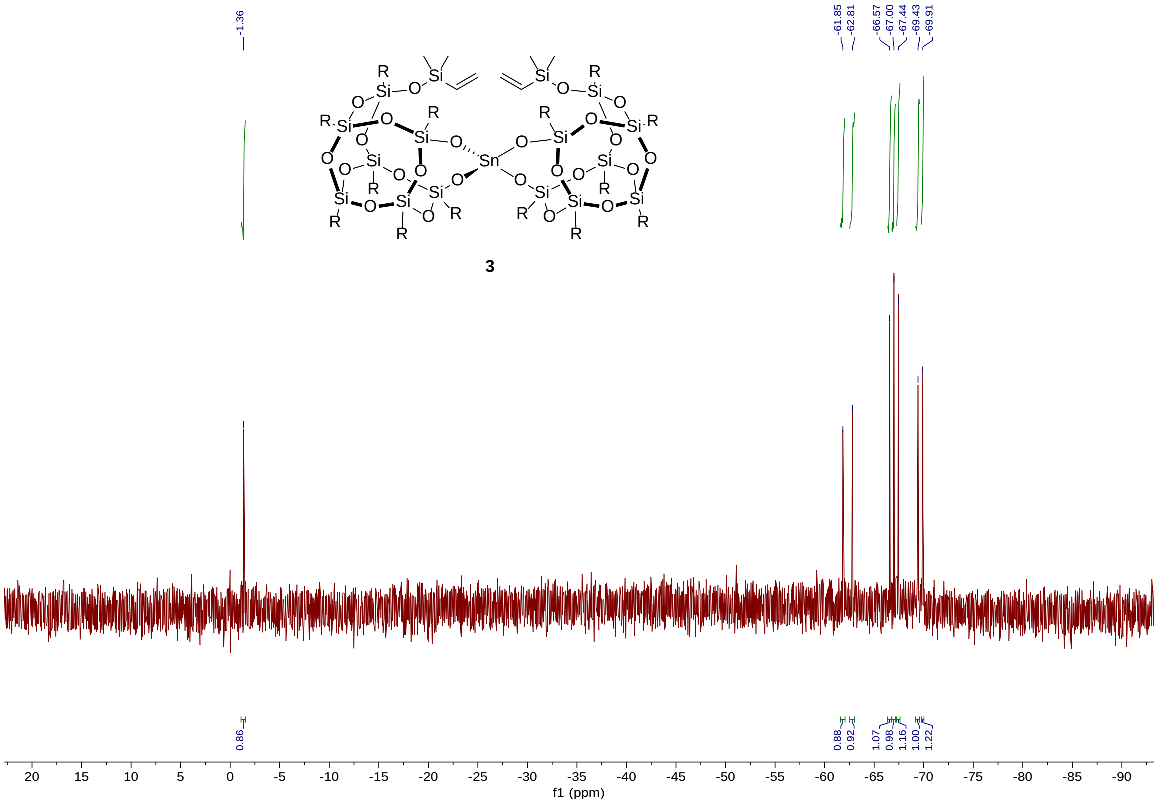

Figure S4c. ^{29}Si NMR spectra of **3** in toluene-d_8.

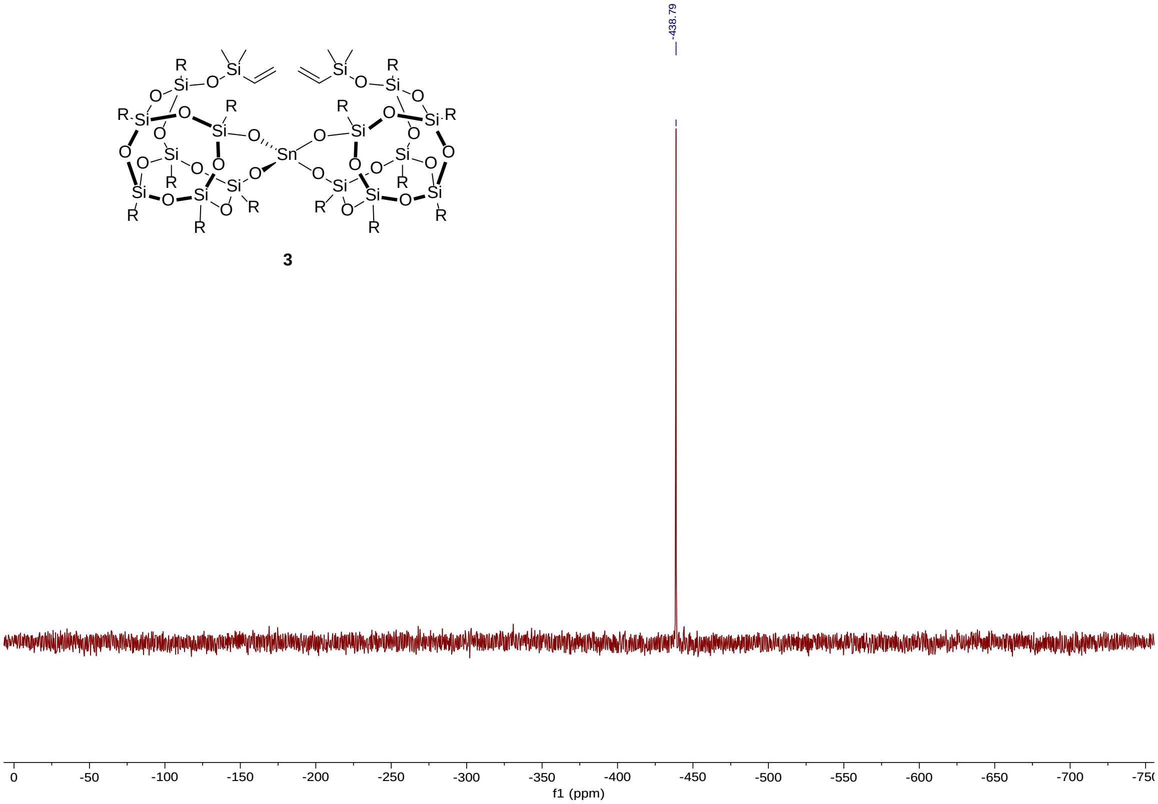

Figure S4d. ^{119}Sn NMR spectra of **3** in toluene-d_8.

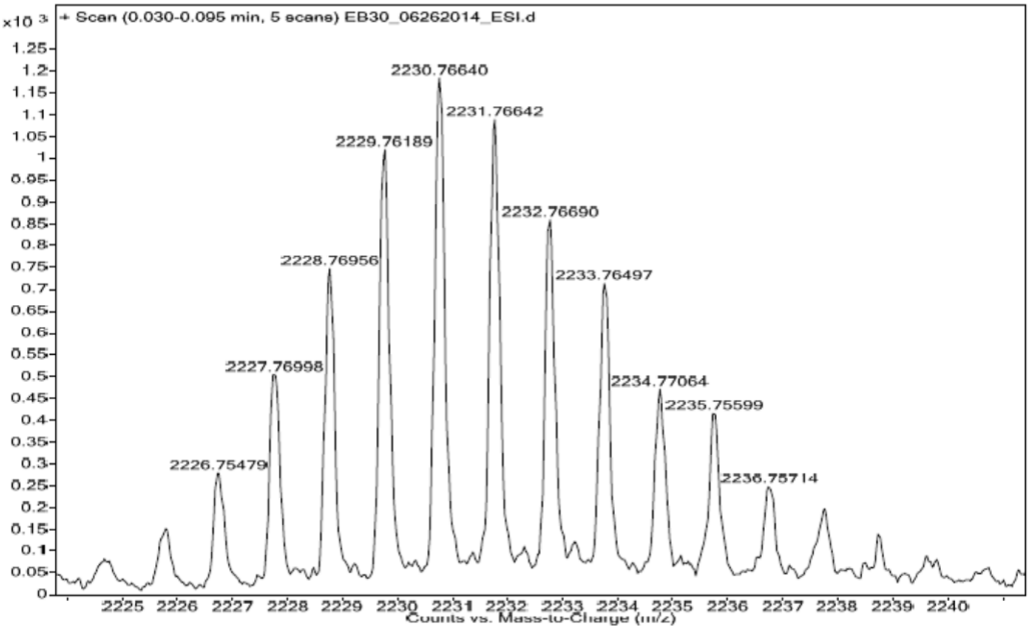

Figure S4e. $(M+H)^+$ peak in the mass spectra of **3** from Figure S4f.

Table S1. Calculated pattern for $C_{92}H_{173}O_{24}Si_{16}Sn$ $(M+H)^+$ in Figure S4f.

m/z	Abundance	*m/z*	Abundance
2221.76673	0.0008842	2233.76649	0.0863146
2222.76845	0.0016524	2234.76689	0.0612804
2223.76780	0.0026308	2235.76726	0.0415084
2224.76774	0.0032961	2236.76770	0.0262558
2225.76447	0.0166177	2237.76802	0.0154313
2226.76546	0.0346393	2238.76828	0.0083409
2227.76518	0.0678069	2239.76845	0.0041271
2228.76574	0.0944530	2240.76849	0.0018625
2229.76560	0.1316717	2241.76831	0.0007567
2230.76608	0.1449128	2242.76796	0.0002666
2231.76618	0.1389505	2243.76728	0.0000769
2232.76640	0.1130863	2244.76592	0.0000149

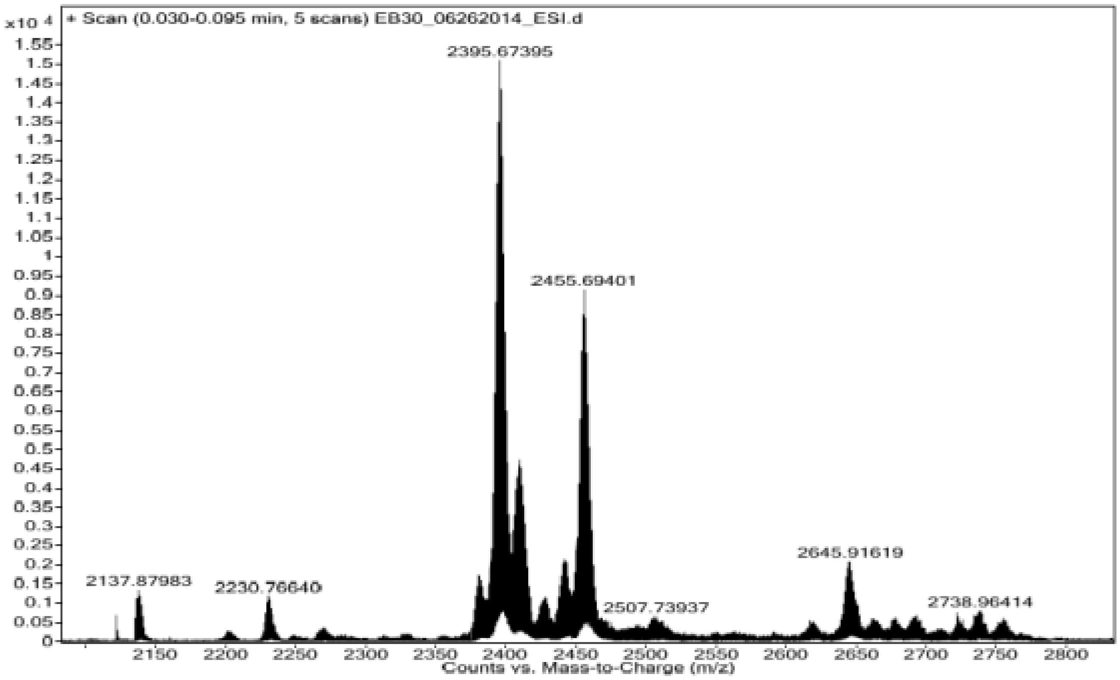

Figure S4f. ESI mass spectra of **3** in CH_2Cl_2. Peak at 2396 assigned to $(M\text{-}Sn^{4+}+3H^{+}\text{-}H_2O+Na^{+}+3CH_2Cl_2)^{+}$ and 2456 to $(M+3H_2O+2CH_2Cl_2)^{+}$.

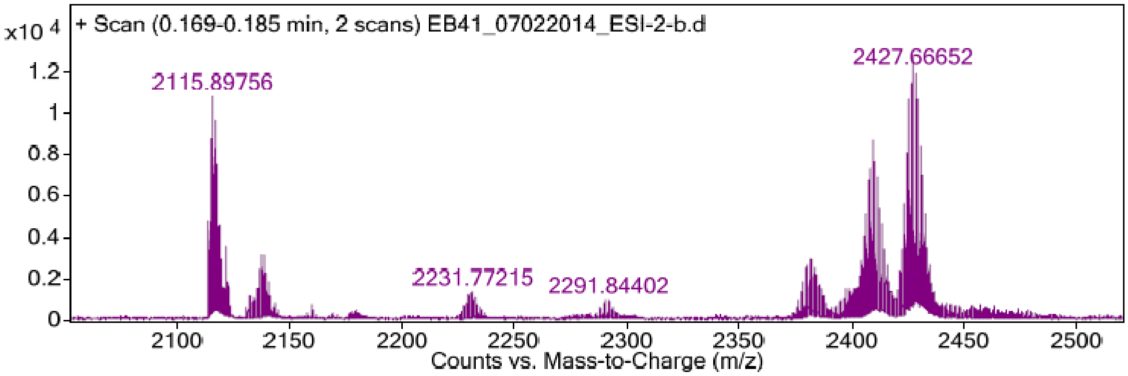

Figure S4g. ESI mass spectra of **3** in $CDCl_3$. Peak at 2115.9 assigned to the loss of tin, and peak at 2427.7 to $(M+3H_2O+CDCl_3+Na)^{+}$ (*m/z* calcd for $C_{93}H_{178}O_{27}Si_{16}SnCl_3DNa$ 2426.70 (100%), 2427.70 (98%)).

Table S2. Edge energies at the Sn K-edge of compound **3** and references. This data is consistent with compound 3 containing Sn(IV).

Sample	**Oxidation state**	**Edge energy (eV)**
Sn foil (for calibration)	0	29200.0
$SnCl_2$	2	29199.4
$SnCl_4$	4	29202.3
SnO_2	4	29203.9
$Sn(O^iPr_4)$	4	29203.8
Compound **3**	4	29203.7

Table S3. Fitted EXAFS data of the samples and references at the Sn K-edge. SnO_2 was used as the reference to fit compound **3** to determine the coordination

Sample	**Measurement**	**Scattering path**	***N***	***R* (Å)**	**$\Delta\sigma^2$**	**E_0 (eV)**
SnO_2 (reference)	Solid, Air	Sn-O	6.0	2.05	N/A	N/A
Compound **3** (fitted using SnO_2 as reference)	Liquid, N_2	Sn-O	4.1	1.93	0.002	-2.4
Compound **3** (fitted using SnO_2 as reference)	Liquid, O_2	Sn-O	4.0	1.93	0.002	-1.8

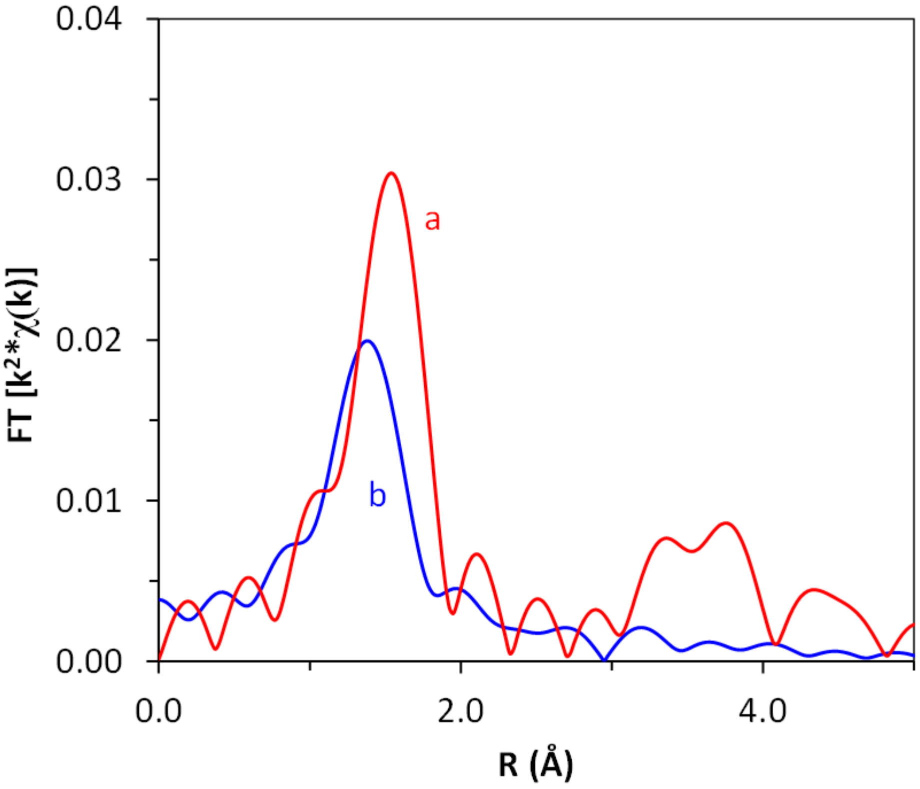

Figure S5a. Sn K-edge magnitude of the FT of the EXAFS of (a) SnO_2 and (b) compound **3** in toluene. k^2: $\Delta k = 2.7\text{-}10.2$ Å^{-1}.

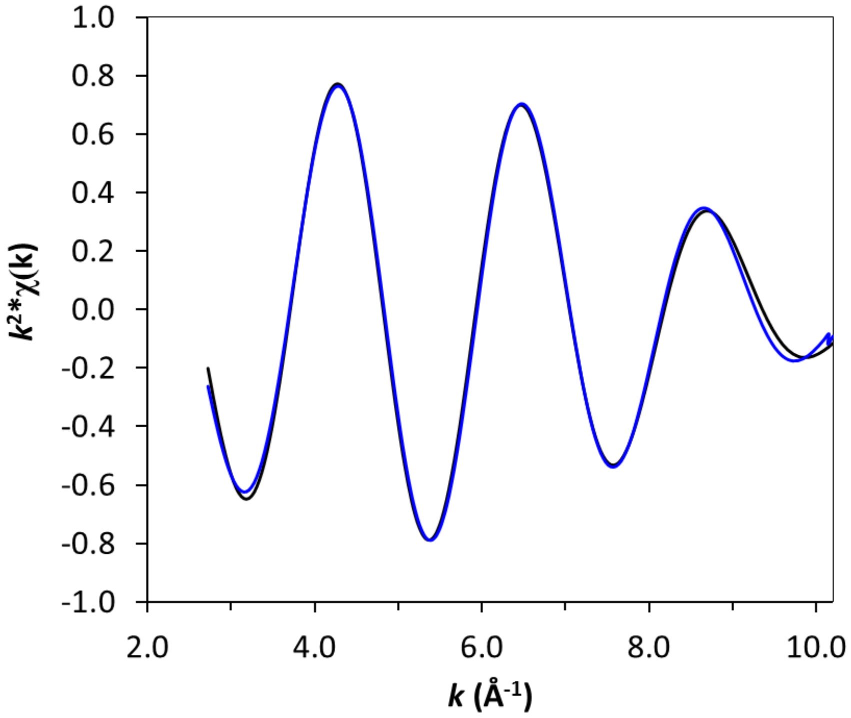

Figure S5b. Sn K-edge k^2 weighted isolated first-shell Fourier transform data and fit of the EXAFS of compound **3** fitted using SnO_2 as the reference. Black: experimental data; blue; fit. k^2: Δk = 2.7-10.2 Å^{-1}. ΔR =1.1-1.8 Å.

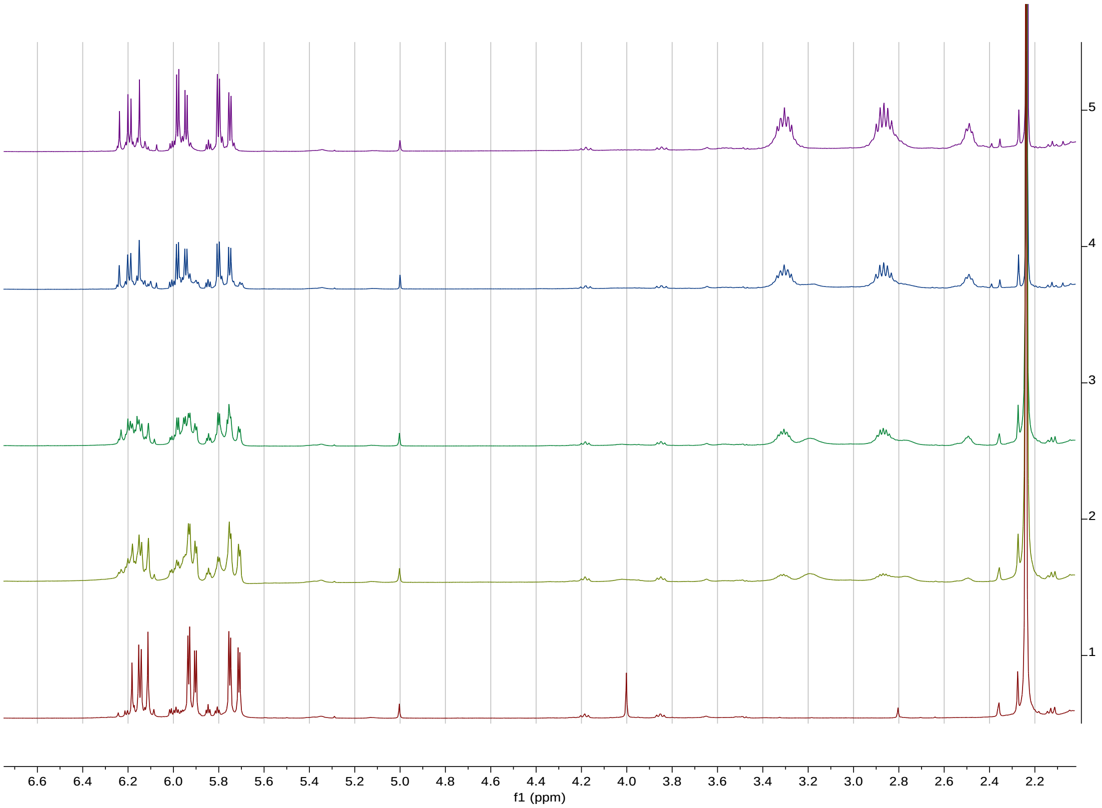

Figure S6a. ^{1}H NMR of **3** after addition of (from bottom to top) 0, 0.5, 1, 1.5 and 2 equivalents of Et_2NH (the resonances of the vinyl protons of **3** (6.2-5.7 ppm), of the two diastereotopic protons of CH_2 (3.31 and 2.84 ppm) and of the NH (2.49 ppm) of **3**-bound Et_2NH are shown).

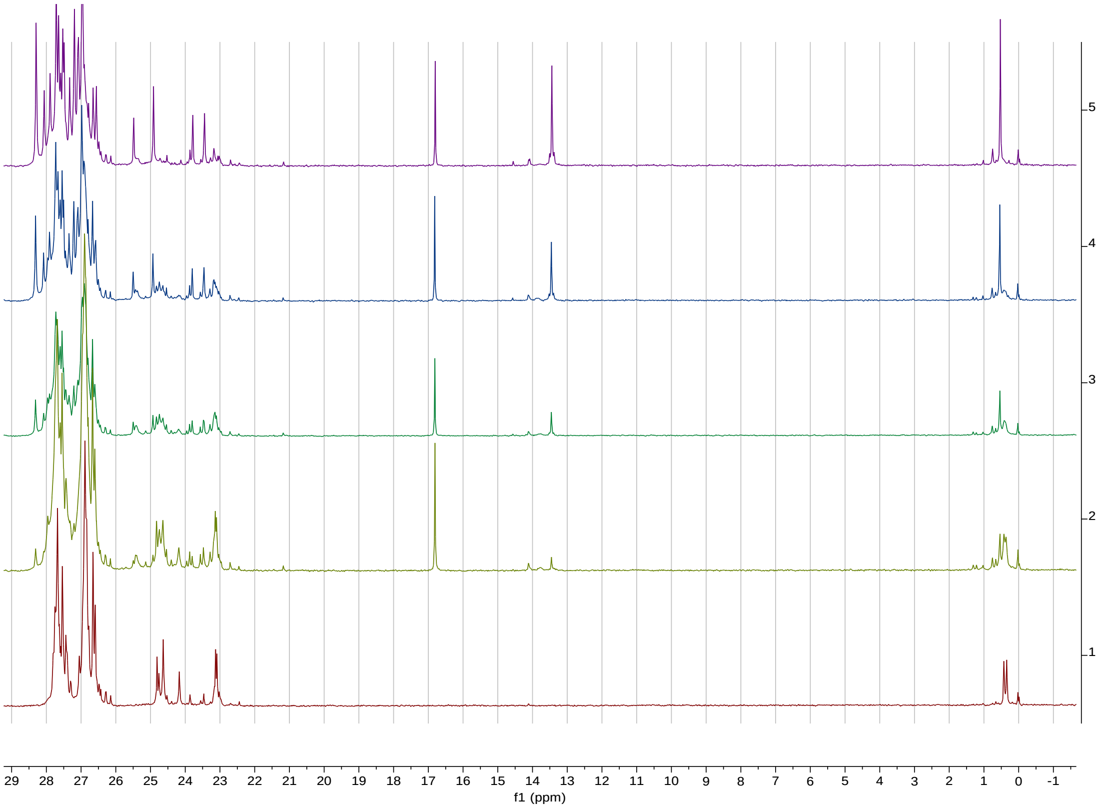

Figure S6b. ^{13}C NMR of **3** after addition of (from bottom to top) 0, 0.5, 1, 1.5 and 2 equivalents of Et_2NH. 7 CH's of *c*-hexyl 24.82, 24.76, 24.64 (2), 24.18, 23.14, 23.10 ppm present in **3** (bottom plot) became 4 peaks (25.50, 24.93, 23.80, 23.46) after addition of two equivalents of Et_2NH (top plot).

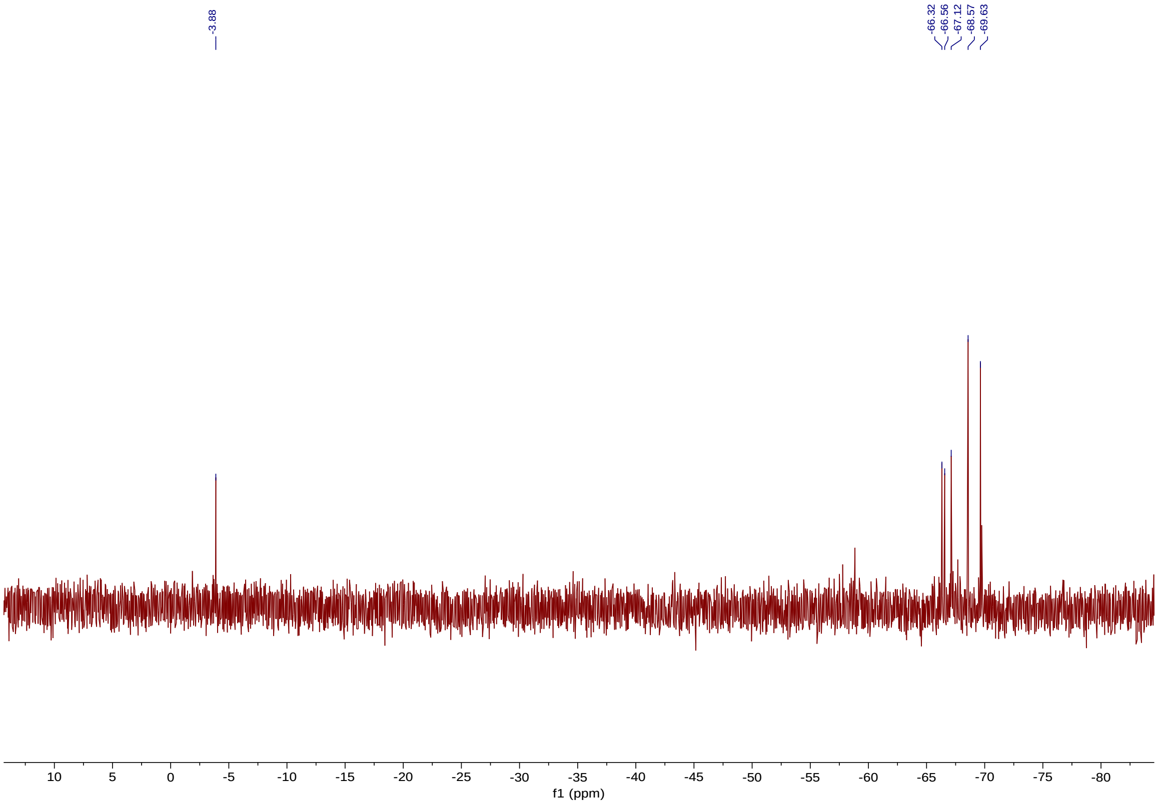

Figure S6c. ^{29}Si NMR of **3** after addition of 2 equivalents of Et$_2$NH.

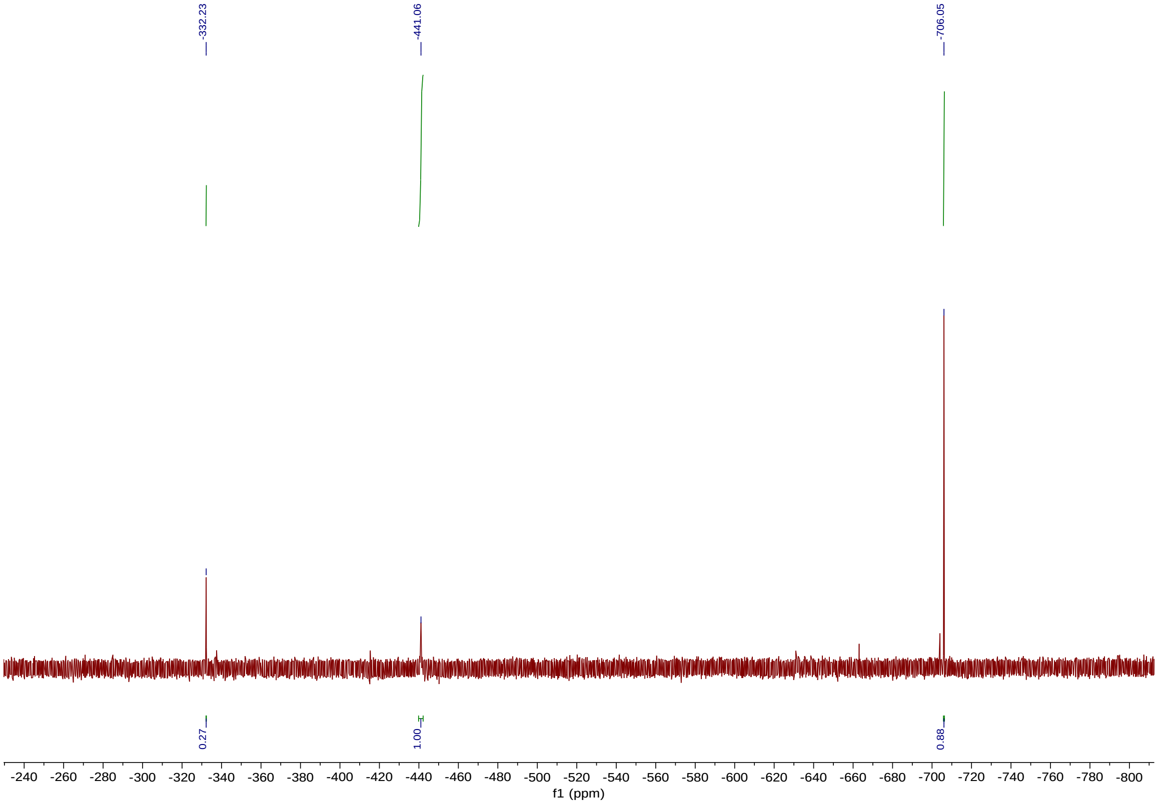

Figure S6d. ^{119}Sn NMR of **3** after addition of 1 equivalent of Et_2NH (-332 ppm is an impurity peak that was present before the addition of Et_2NH and accounted for 12% of the total integrated intensity of the Sn peaks).

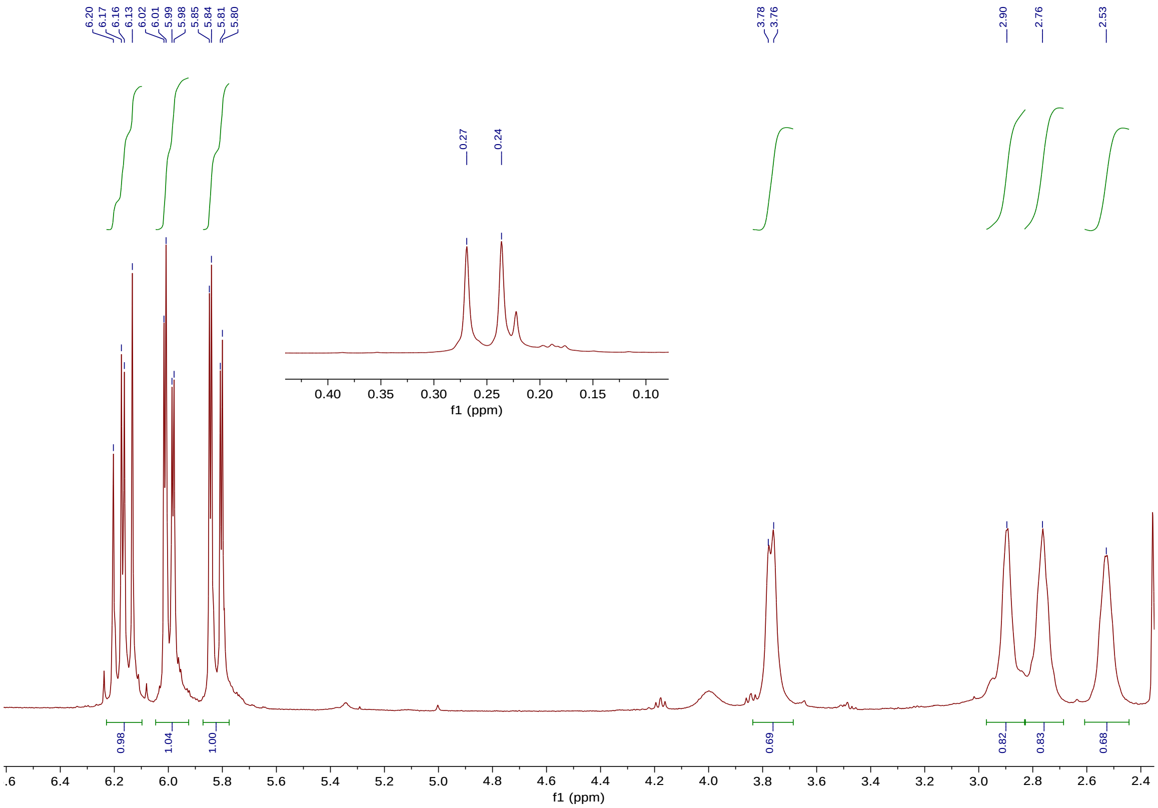

Figure S7a. ^{1}H NMR of **3** after addition of 1 equivalent of ethylenediamine (the signals of the vinyl (6.2-5.8 ppm), methyls (inset) and the two pairs of diastereotopic protons of CH$_2$'s and NH$_2$'s (3.8-2.4 ppm) of **3**•$H_2NCH_2CH_2NH_2$ are shown).

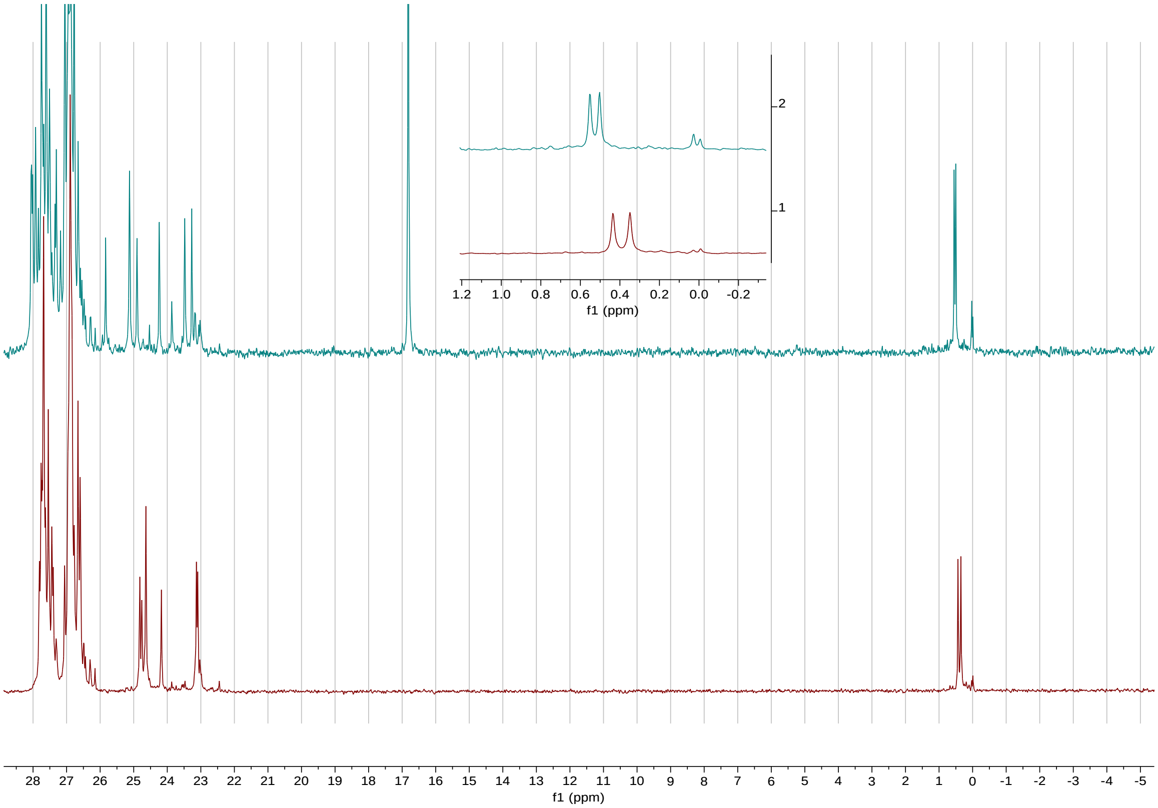

Figure S7b. ^{13}C NMR of **3** after addition of 1 equivalent of ethylenediamine. Seven peaks are observed (two overlap) in the CH (26-23 ppm) and two in the methyl (*ca.* 0 ppm) regions.

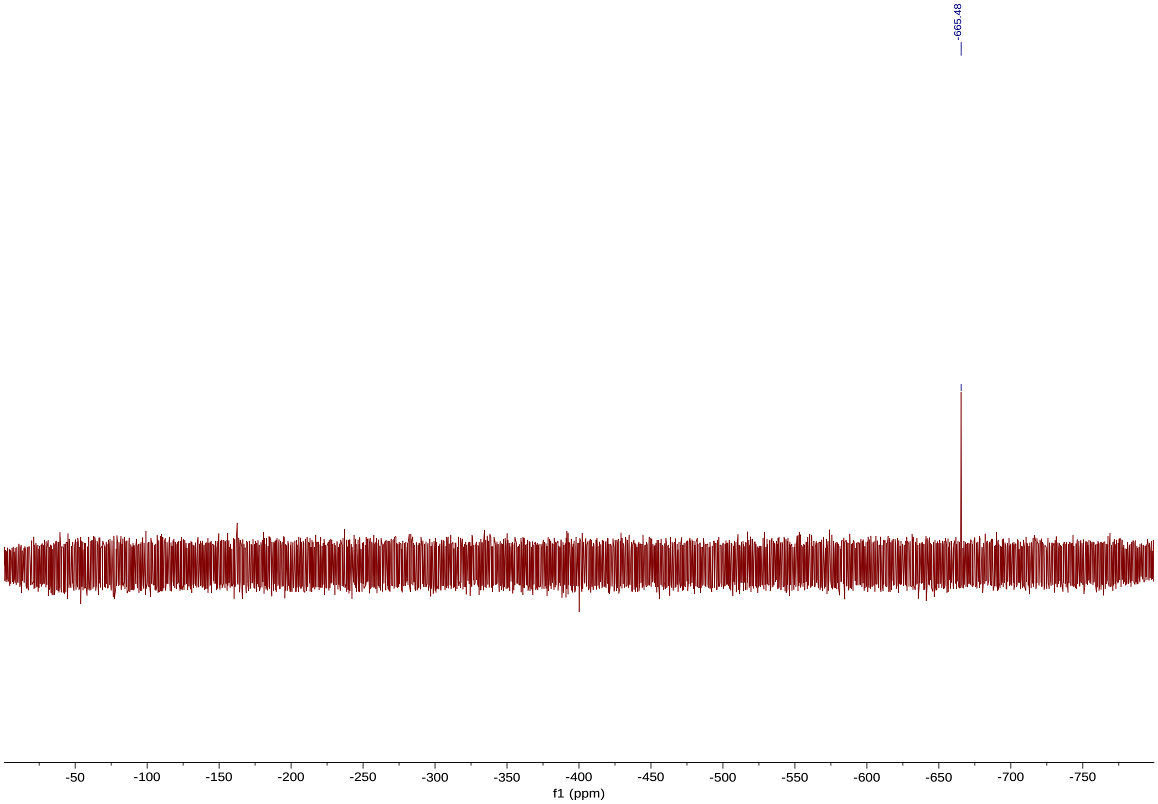

Figure S7c. ^{119}Sn NMR of **3** after addition of 1 equivalent of ethylenediamine.

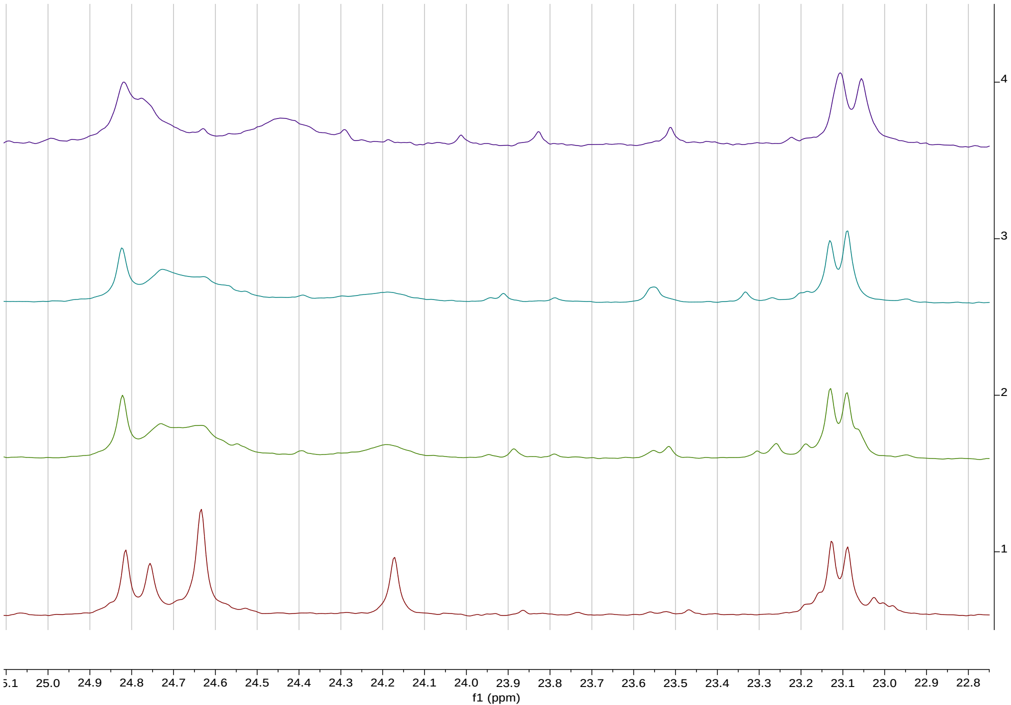

Figure S8a. Expanded CH-region of the ^{13}C NMR of **3** after addition of (from bottom to top) 0, 1, 2, and 32 equivalents of Et_3N.

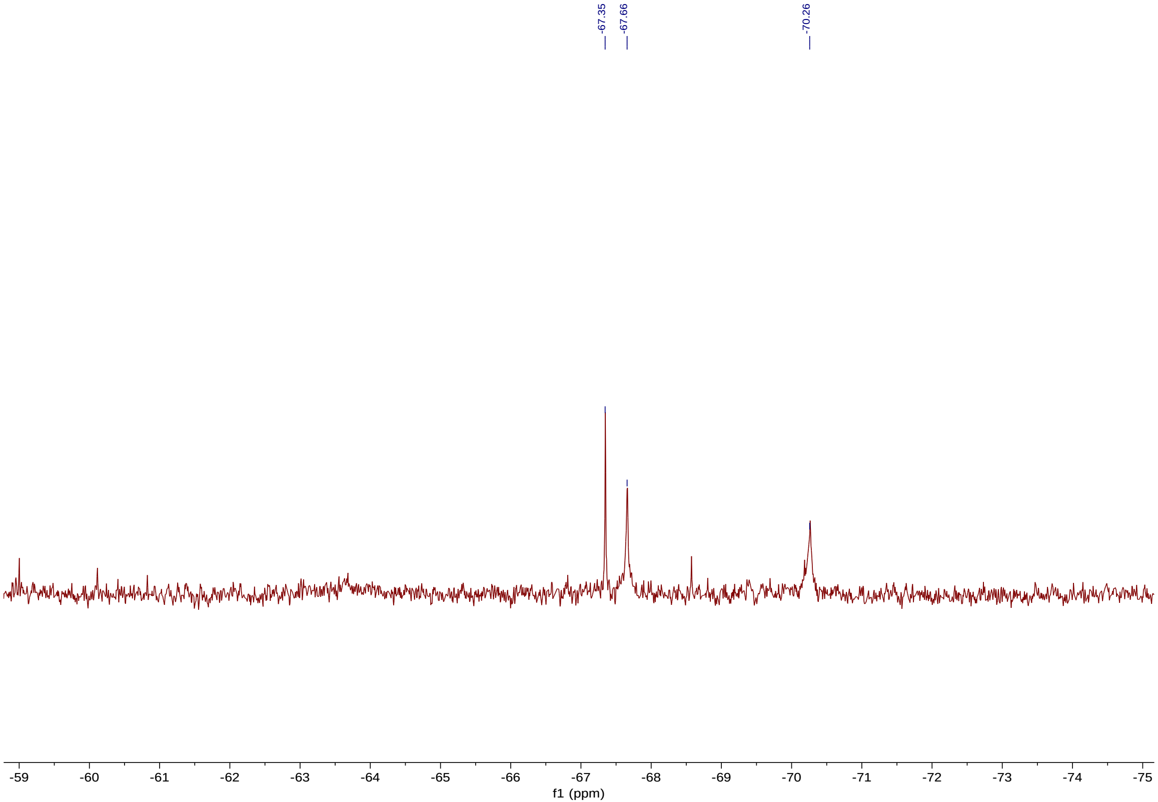

Figure S8b. The POSS-region expansion of the ^{29}Si NMR of **3** after the addition of 32 eq. of Et_3N (all except three signals broadened or disappeared).

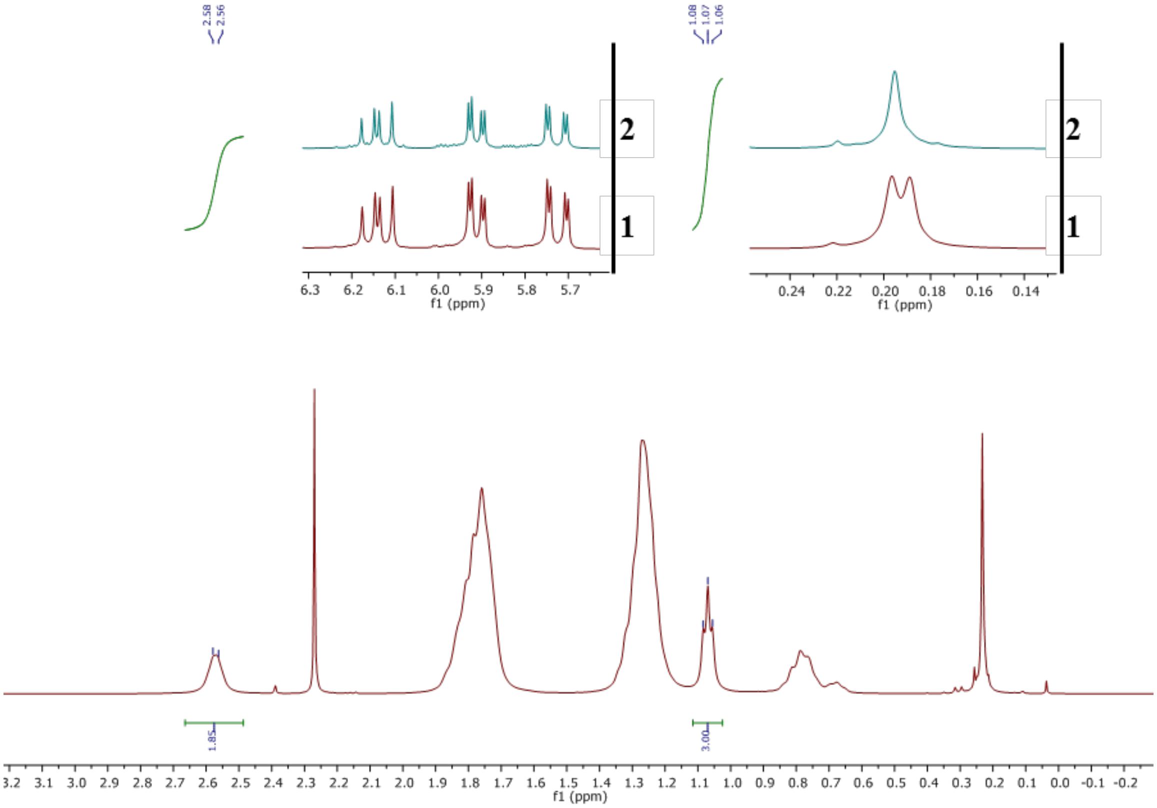

Figure S8c. ^{1}H NMR expansion of **3** upon addition of 2 equivalents of Et_3N. Broadened CH_2 signal of triethylamine is at 2.6 ppm. Insets show comparison of vinyl and methyl regions without (1) and with (2) the base, indicating no noticeable change.

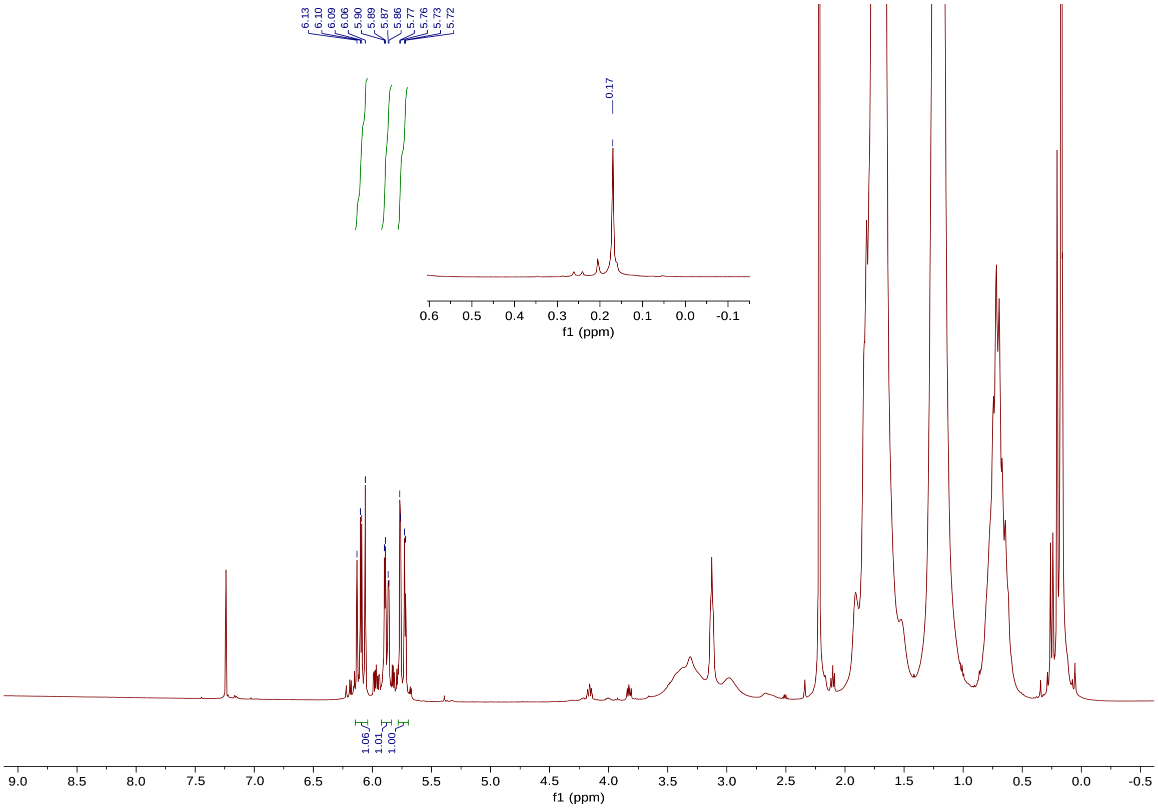

Figure S9a. ^{1}H NMR of **3** after addition of 1 equivalent of 1,8-Diazabicyclo[5.4.0]-undec-7-ene, and hexamethylbenzene (internal standard). Insert: coalescence of methyl groups resonances.

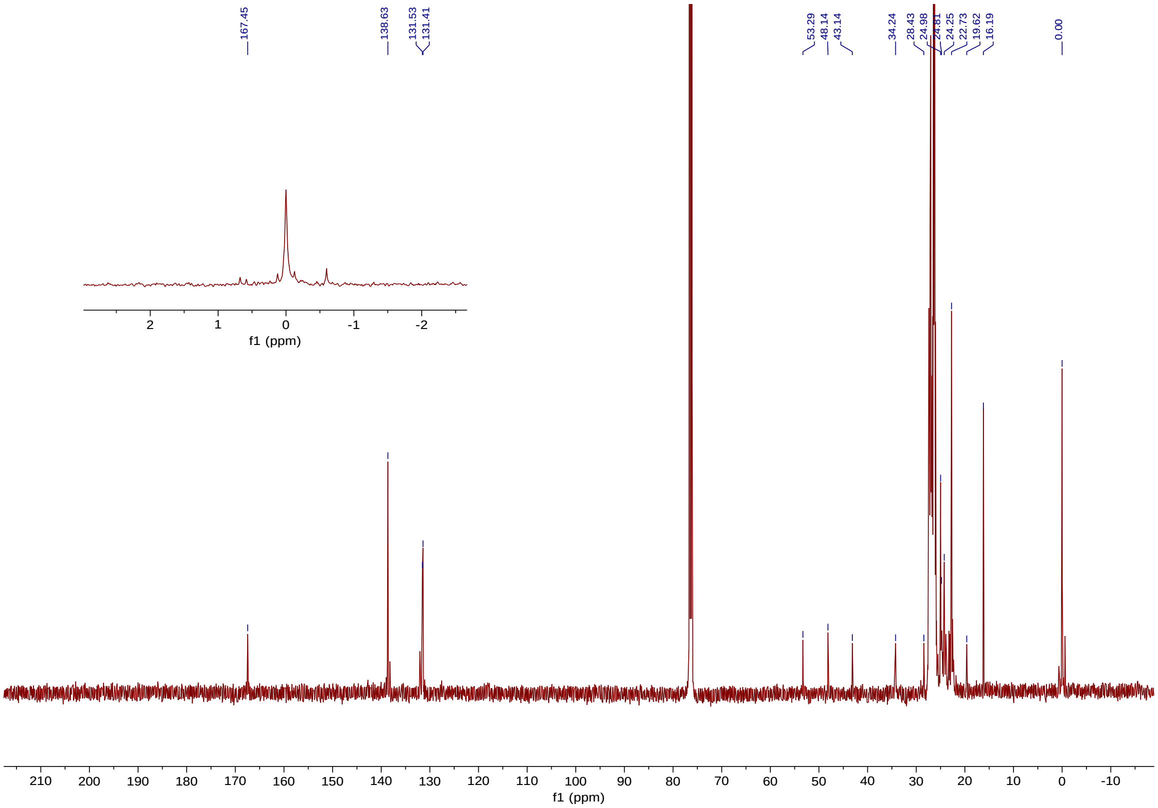

Figure S9b. ^{13}C NMR of **3** after addition of 1 equivalent of 1,8-Diazabicyclo[5.4.0]-undec-7-ene, and hexamethylbenzene (internal standard). Upon addition of another equivalent of DBU, additional signals representing free DBU appeared. Insert: coalescence of methyl groups resonances.

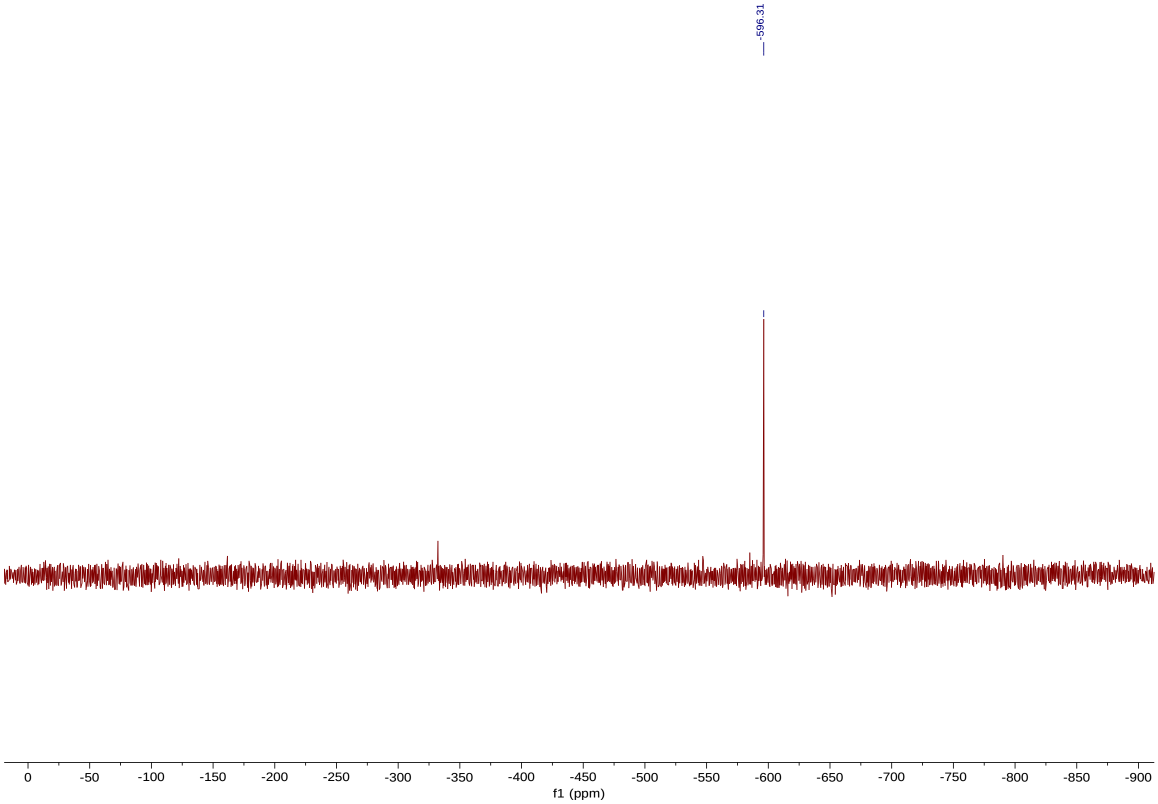

Figure S9c. ^{119}Sn NMR of **3** after addition of 2 equivalents of 1,8-Diazabicyclo[5.4.0]-undec-7-ene.

References

1. K.-Y. Ko, E. L. Eliel, *J. Org. Chem.* **1986**, *51*, 5353–5362.
2. A.A. Bolzan, C. Fong, B.J. Kennedy, C.J. Howard. Acta Crystallogr. B **1997**, *53*, 373–380.